The Far-Infrared Laser Magnetic Resonance Spectrum of the CD Radical and Determination of Ground State Parameters[1]

JOHN M. BROWN

The Physical Chemistry Laboratory, South Parks Road, Oxford OX1 3QZ, England

AND

KENNETH M. EVENSON

National Institute of Standards and Technology, Boulder, Colorado 80303

The far-infrared laser magnetic resonance spectrum of the CD radical in the $v = 0$ level of the $X^2\Pi$ state has been studied in detail. Twelve transitions which are accessible with currently available laser lines have been recorded. The measurements have been analyzed and subjected to a single least-squares fit using an effective Hamiltonian. The data provide primary information on the rotational and fine-structure intervals between the lowest rotational intervals. They also yield values for the Λ-type doubling and deuteron hyperfine splittings in the same levels. Combination of the measurements with the corresponding data for CH allows the two parameters, γ and A_D, to be determined separately. © 1989 Academic Press, Inc.

1. INTRODUCTION

The significance of the CH radical as a chemical species has long been appreciated (*1*). It plays an important role in hydrocarbon combustion processes (*2*) and also in chemi-ionization (*3*). It also plays a significant part in interstellar chemistry (*4*). From a spectroscopic point of view, its energy levels are now very well characterized, based on a variety of measurements which include electronic (*5–8*), infrared (*9, 10*), far-infrared (*11, 12*), and microwave spectroscopy (*8, 13*). Recently, the microwave and far-infrared measurements have been extended to ^{13}CH (*14, 15*) with the primary objective of defining the electronic wavefunction in the region of the carbon nucleus. By comparison, rather little is known about the deuterated isotopomer, CD. Only its electronic spectrum has been studied, first by Gerö (*16*) and later by Herzberg and Johns (*6*). Although these studies served to locate several electronic states of CD, they provide only rather imprecise structural information. The experimental data were of low precision which limited the interpretation of the results.

There are several reasons why it is worthwhile to study CD. First, not all its properties are easily predictable from those of CH. For example, the combination of measurements for CD with those for CH allows the separation of the two parameters, γ and A_D (*17*) which describe spin–rotation coupling and the centrifugal distortion of spin–orbit coupling, respectively. For each isotopomer on its own, only a single effective parameter

is determinable which is a linear combination of the two. Furthermore, a more detailed study of CD provides reliable measurements of the lambda-doubling intervals which can be used by radio-astronomers in a search for CD in the interstellar medium. There is also a pedagogic reason for studying CD in more detail. By an accident of nature, its spin–orbit coupling parameter A is almost exactly four times its rotational constant B and, as a result, its energy levels conform almost perfectly to Hund's case (b) (1).

In this paper, we report the measurement of the far-infrared laser magnetic resonance (LMR) spectrum of CD in its ground vibrational level. The data set is extensive and has been used to determine the parameters of an effective Hamiltonian for a molecule in a $^2\Pi$ state. The implications of these results for a more detailed understanding of CH itself are discussed.

2. EXPERIMENTAL DETAILS

The spectra were recorded at the Boulder laboratories of the NIST with a far-infrared LMR spectrometer which has been described in detail elsewhere (18). The CD radicals were produced in the spectrometer sample volume by the reaction of fluorine atoms with deuterated methane in a flow system, the fluorine atoms being generated by passing a 10% mixture of F_2 in He through a microwave discharge. This is the same method that was used to generate CH (11, 12). The total pressure in the sample region was about 250 mTorr (33 Pa) which permitted Lamb dips to be observed on all the strong lines. The magnet of the LMR spectrometer was controlled by a rotating coil system which provided a direct readout of the flux densities. The system was calibrated periodically up to 1.8 T with a proton NMR gaussmeter; the absolute uncertainty was 10^{-5} below 0.1 T and the fractional uncertainty was 10^{-4} above 0.1 T.

The observed far-infrared LMR spectrum of the CD radical in the $v = 0$ level of the A $^2\Pi$ state is summarized in Table I. Twelve rotational transitions in CD have been observed using nine laser lines, as shown in the energy level diagram of Fig. 1. The signal-to-noise ratios were very good, of the order of 1000:1 for the strongest lines with a 300 msec output time constant. For example, the low field portion of the spectrum recorded with the 215.4-μm laser line in parallel polarization ($\Delta M_J = 0$), arising from the transition $N = 3 \leftarrow 2$, $J = 2\frac{1}{2} \leftarrow 1\frac{1}{2}$ is shown in Fig. 2. Lamb dips can be seen clearly on the resonance at 32 mT. Several transitions of CD_2 were recorded under the same conditions. These spectra have, for the most part, been analyzed and published elsewhere (19, 20).

3. ASSIGNMENT AND FITTING

3.1. Hund's Case (b) Behavior for a Molecule in a $^2\Pi$ State with $A = 4B$

The rotational energy levels for a molecule in a $^2\Pi$ state with $A \simeq 4B$ follow Hund's case (b) behavior exactly. This can be appreciated from a consideration of the simple 2×2 matrix representation for a given J-value of the spin–orbit coupling and the rotational kinetic energy:

$$H_{so} + H_{rot} = AL_zS_z + B(\mathbf{J} - \mathbf{S})^2. \tag{1}$$

Despite the objective of describing case (b) behavior, it is easier and more familiar to

TABLE I

Summary of Observations in the Far-Infrared LMR Spectrum of the CD Radical in Its Ground State

	Laser line			CD transition		
Pump	Gain medium	$\lambda/\mu m$	ν/GHz[a]	N	J	F_i
10R(16)	C_2H_3Br	680.5	440.5205	$1 \leftarrow 1$	$1\tfrac{1}{2} \leftarrow \tfrac{1}{2}$[b]	$F_1 \leftarrow F_2$
9P(36)	CH_2DOH	336.2	891.5863 ⎫	$2 \leftarrow 1$	$1\tfrac{1}{2} \leftarrow 1\tfrac{1}{2}$	$F_2 \leftarrow F_1$
9P(22)	$^{13}CH_3OH$	339.0	884.4381 ⎭			
9R(14)	CH_2F_2	326.4	918.4170	$2 \leftarrow 1$	$2\tfrac{1}{2} \leftarrow 1\tfrac{1}{2}$	$F_1 \leftarrow F_1$
10R(38)	CD_2F_2	218.3	1373.5133	$3 \leftarrow 2$	$3\tfrac{1}{2} \leftarrow 2\tfrac{1}{2}$	$F_1 \leftarrow F_1$
					$2\tfrac{1}{2} \leftarrow 2\tfrac{1}{2}$	$F_2 \leftarrow F_1$
9R(14)	CH_3OD	215.4	1391.9721	$3 \leftarrow 2$	$2\tfrac{1}{2} \leftarrow 1\tfrac{1}{2}$	$F_2 \leftarrow F_2$
10R(38)	CH_3OH	163.0	1838.8393	$4 \leftarrow 3$	$4\tfrac{1}{2} \leftarrow 3\tfrac{1}{2}$	$F_1 \leftarrow F_1$
					$3\tfrac{1}{2} \leftarrow 2\tfrac{1}{2}$	$F_2 \leftarrow F_2$
10R(34)	CH_3OH	129.5	2314.1113	$5 \leftarrow 4$	$5\tfrac{1}{2} \leftarrow 4\tfrac{1}{2}$	$F_1 \leftarrow F_1$
					$4\tfrac{1}{2} \leftarrow 3\tfrac{1}{2}$	$F_2 \leftarrow F_2$
9P(12)	CH_2DOH	108.8	2754.9957	$6 \leftarrow 5$	$6\tfrac{1}{2} \leftarrow 5\tfrac{1}{2}$	$F_1 \leftarrow F_1$
					$5\tfrac{1}{2} \leftarrow 4\tfrac{1}{2}$	$F_2 \leftarrow F_2$

[a] Frequencies taken from Inguscio *et al.* (*28*).
[b] The level $J = \tfrac{1}{2}$ is a unique level and only formally described as the F_2 component of the $N = 1$ level for CD.

formulate the problem in a case (a) basis set. The matrix in this case is given in Table II and its eigenvalues are

$$E_\pm = B(J + \tfrac{1}{2})^2 \pm \tfrac{1}{2}[(A - 2B)^2 + 4B^2\{(J + \tfrac{1}{2})^2 - 1\}]^{1/2}. \tag{2}$$

In the true case (b) limit, with $A = 0$, the eigenvalues are

$$E_\pm = B(J + \tfrac{1}{2})^2 \pm B(J + \tfrac{1}{2}) \tag{3}$$

which can be expressed in a more recognizable form by introducing the case (b) quantum number N,

$$F_1, \qquad J = N + \tfrac{1}{2}: \qquad E_- = BN(N + 1) \tag{4a}$$

$$F_2, \qquad J = N - \tfrac{1}{2}: \qquad E_+ = BN(N + 1). \tag{4b}$$

These are the familiar case (b) expressions (*1*) and, to this order of approximation, there is no fine structure splitting. However, exactly the same result is obtained for $A = 4B$ as can be appreciated by looking at the expression under the square root in Eq. (2). From the point of view of the energy levels, it is not possible to distinguish
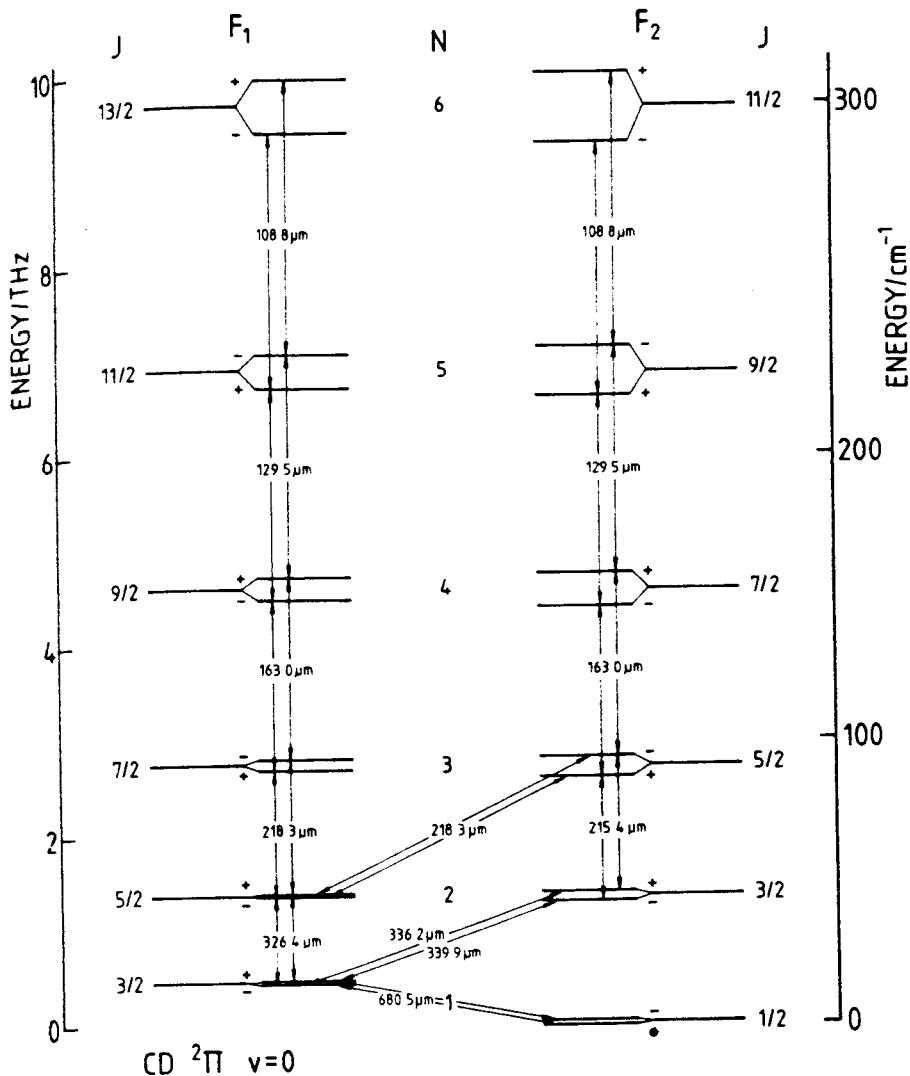
FIG. 1. Diagram showing the lower rotational levels of the CD radical in its $X^2\Pi$ state and the observed transitions involved in the observed far-infrared LMR spectrum. Note the goodness of the case (b) quantum number N: i.e., the spin-rotation splitting is very small. The Λ-type (parity) doubling has been exaggerated by a factor of 20 for clarity.

between a molecule with $A = 4B$, such as CD, and a true Hund's case (b) molecule with $A = 0$. The variation of $^2\Pi$ energy levels with A shows a symmetrical behavior about $A = 2B$. This has been realized by many authors in the past (21, 1, 22, 23, 24). However, it does not appear to be so widely appreciated that the cases $A = 0$ and $A = 4B$ are easily distinguished in practice because the corresponding eigenfunctions are different,

$$|+\rangle = \cos \beta |1\rangle + \sin \beta |2\rangle \tag{5a}$$
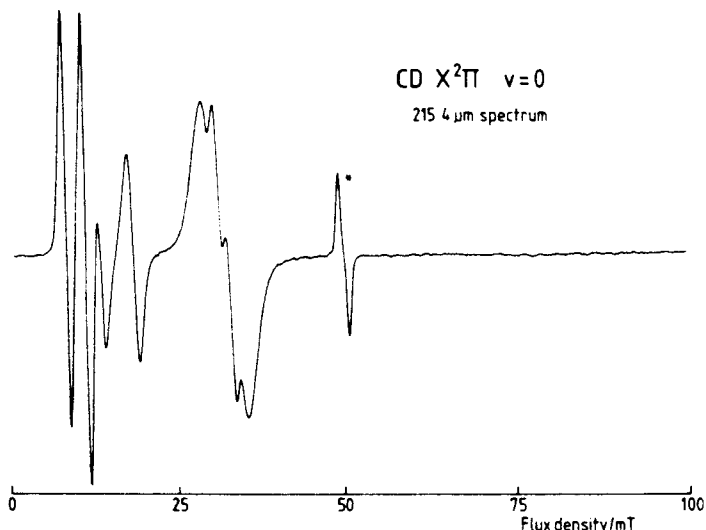
$$|-\rangle = -\sin \beta |1\rangle + \cos \beta |2\rangle, \tag{5b}$$

FIG. 2. The low-field portion of the 215.4 μm LMR spectrum of the CD radical in parallel polarizati (π or $\Delta M_J = 0$). The rotational transition involved is $N = 3 \leftarrow 2$, $J = 5/2 \leftarrow 3/2$. Note the promine Lamb dips on the line at 32 mT arising from the deuteron hyperfine splitting. The line marked with ‿ asterisk also shows a triplet structure at lower modulation but does not arise from CD in the $v = 0$, 1, or levels.

where

$$\left. \begin{array}{l} \sin 2\beta = \dfrac{-2Bz^{1/2}}{[(A - 2B)^2 + 4B^2z]^{1/2}} = \dfrac{-z^{1/2}}{(J + \frac{1}{2})} \\[4mm] \cos 2\beta = \dfrac{(A - 2B)}{[(A - 2B)^2 + 4B^2z]^{1/2}} = \dfrac{1}{(J + \frac{1}{2})} \end{array} \right\} \quad \text{for} \quad A = 4B.$$

For $A = 0$, the result is the same for $\sin 2\beta$ but has the opposite sign for $\cos 2\beta$. Th molecular observables which depend on the phase of the eigenfunctions, such as tra sition intensities and magnetic dipole moments will differ in the two cases. The magnet

TABLE II

Matrix Representation for a Given J Value of the Spin–Orbit Coupling and
the Rotational Kinetic Energy of a Molecule in a $^2\Pi$ State

$\frac{1}{2}A + Bz$	$-Bz^{\frac{1}{2}}$
$-Bz^{\frac{1}{2}}$	$-\frac{1}{2}A + B(z + 2)$

Note. A Hund's case (a) basis set has been used to construct the matrix. The first row (or column) ret
to the $^2\Pi_{3/2}$ component and the second to the $^2\Pi_{1/2}$ component. The quantity z is equal to $(J + \frac{1}{2})^2 - $

moments are of direct importance to the present work. The g-factors calculated for the two cases considering only the major contributions, from the electron spin and orbital magnetic moments, are given in Table III. It is obvious that a measurement of the Zeeman splitting will clearly distinguish between the cases $A = 0$ and $A = 4B$. The values for the intermediate case, $A = 2B$, to which CH itself closely corresponds, are also given for comparison in Table III. The manner in which CD shows Hund's case (b) behavior can be seen in the energy level diagram of Fig. 1. It can be seen from this figure that almost all the possible transitions between low-lying levels of CD have been detected. The notable exception is $N = 2$, $J = \frac{3}{2} \leftarrow J = \frac{1}{2}$. Reference to Table III shows that the g-factors for both these levels are quite small and the transition between them therefore tunes only slowly with magnetic field. There was not a usable far-infrared laser line close enough in frequency to enable it to be detected.

3.2. Analysis

The LMR spectra of the CD radical were assigned with the help of a predictive computer program which we have used in our earlier studies of molecules in $^2\Pi$ states, e.g., Ref. (12). In the initial calculations, use was made of the optical B value together with parameters scaled from those of CH using the appropriate isotopic factor. The simulated magnetic resonance spectra obtained from these calculations were usually similar enough to the observed to permit the assignments to be made directly. The full details of the experimental measurements and their assignments are given in Table IV. For the most part, the transitions obey the expected selection rule $\Delta M_J = 0$ (π polarization) or ± 1 (σ) and $\Delta M_I = 0$. In addition, a number of weaker transitions which are formally forbidden ($\Delta M_I = \pm 1$) were observed at low fields where the nuclear spin is still partially coupled to the electronic angular momenta. The transitions in CD for which Lamb dips were observed are marked in Table IV with a superscript d.

TABLE III

First-Order g-Factors g_J for Molecules in near Hund's Case (b) $^2\Pi$ States

J	A = 0 F_1	F_2	A = 2B F_1	F_2	A = 4B F_1	F_2
½	...	−0.0007	...	−0.0007	...	−0.0007
1½	1.0008	−0.2005	0.8625	−0.0622	0.6000	0.2000
2½	0.5338	−0.1908	0.4951	−0.1521	0.4191	−0.0762
3½	0.3575	−0.1669	0.3414	−0.1509	0.3095	−0.1191
4½	0.2669	−0.1457	0.2588	−0.1375	0.2424	−0.1212
5½	0.2123	−0.1284	0.2076	−0.1237	0.1981	−0.1142

Note. The Zeeman energy is expressed as $g_J \mu_B B_0 M_J$. In its ground $X^2\Pi$ state, CH corresponds closely to $2B$ and CD to $A = 4B$.

TABLE IV

Measurements and Assignments of Transitions Observed by Far-Infrared LMR for CD in the $V^2\Pi$ State

parity	M_J	M_I^a	Flux Density (mT)	$\nu_{laser} - \nu_{calc}$ (MHz)	W_t^b (MHz^{-2})	$\partial\nu/\partial B_0^c$ (MHz/G)

680.5 μm spectrum N=1, J=1½ ← J=½

‖-polarisation (π)

parity	M_J	M_I^a	Flux Density (mT)	$\nu_{laser} - \nu_{calc}$ (MHz)	W_t^b (MHz^{-2})	$\partial\nu/\partial B_0^c$ (MHz/G)
− ← +	½ ← −½	−1 ← 0	157.28	−0.8	10.30	0.46
− ← +	½ ← ½	−1	158.47	0.1	10.30	0.46
− ← +	½ ← ½	0	158.95	−0.2	5.00	0.46
− ← +	½ ← ½	1	159.38	−0.3	10.30	0.46
+ ← −	½ ← ½	−1	271.10	−0.1	5.00	0.47
+ ← −	½ ← −½	0 ← 1	271.10	0.3	5.00	0.47
+ ← −	½ ← ½	1	274.25	1.0	5.00	0.47
+ ← −	½ ← ½	0	274.44	0.9	5.00	0.47
+ ← −	½ ← −½	−1 ← 0	274.71	0.4	5.00	0.47

⊥-polarisation (σ)

parity	M_J	M_I^a	Flux Density (mT)	$\nu_{laser} - \nu_{calc}$ (MHz)	W_t^b (MHz^{-2})	$\partial\nu/\partial B_0^c$ (MHz/G)
− ← +	½ ← ½	0 ← −1	52.71	0.8	10.30	1.36
− ← +	1½ ← ½	−1	52.94	0.4	10.30	1.36
− ← +	1½ ← ½	0	53.21	0.6	10.30	1.35
− ← +	1½ ← ½	1	53.46	0.9	10.30	1.35
− ← +	½ ← −½	e	157.67	0.0	10.30	0.46
+ ← −	½ ← −½	1	271.51	0.0	10.30	0.47
+ ← −	½ ← −½	0	275.31	−0.8	10.30	0.47
+ ← −	½ ← −½	−1	nm		0.0	0.47

336.2 μm spectrum N = 2, J = 1½ ← N = 1, J = 1½

‖-polarisation (π)

parity	M_J	M_I^a	Flux Density (mT)	$\nu_{laser} - \nu_{calc}$ (MHz)	W_t^b (MHz^{-2})	$\partial\nu/\partial B_0^c$ (MHz/G)
+ ← −	−1½ ← −1½	−1	488.91	0.6	2.516	0.74
+ ← −	−1½ ← −1½	0	490.27	0.8	2.516	0.74
+ ← −	−1½ ← −1½	1	491.63	1.0	2.516	0.74
− ← +	−1½ ← −1½	−1	871.63	−0.7	2.516	0.53
− ← +	−1½ ← −1½	0	872.30	−0.9	2.516	0.53
− ← +	−1½ ← −1½	1	872.94	−1.0	2.516	0.53

[a] Most of the observed transitions obey the selection rule $\Delta M_I = 0$.

[b] The weights used in the least-squares fit are estimated from the inverse square of the estimated experimental uncertainty of each data point.

[c] Tuning rate computed using the parameter values given in Table V.

[d] Measurement made on a Lamb dip.

[e] Deuteron hyperfine splitting not resolved.

TABLE IV—*Continued*

parity	M_J	M_I[a]	Flux Density (mT)	$\nu_{laser} - \nu_{calc}$ (MHz)	Wt[b] (MHz^{-2})	$\partial\nu/\partial B_0$[c] (MHz/G)
. polarisation (σ)						
. + -	$-\frac{1}{2} \leftarrow -1\frac{1}{2}$	-1	405.27	-0.1	2.516	0.91
. + -	$-\frac{1}{2} \leftarrow -1\frac{1}{2}$	0	405.81	0.1	2.576	0.91
. + -	$-\frac{1}{2} \leftarrow -1\frac{1}{2}$	1	406.37	0.2	2.516	0.91
. + +	$-\frac{1}{2} \leftarrow -1\frac{1}{2}$	e	701.18	-1.3	2.516	0.72

$\square 9.0~\mu m$ *spectrum* $N = 2$, $J = 1\frac{1}{2} \leftarrow N = 1$, $J = 1\frac{1}{2}$

1 polarisation (π)						
+ +	$\frac{1}{2} \leftarrow 1\frac{1}{2}$	$0 \leftarrow 1$	26.74	-0.6	1.278	-1.27
+ +	$\frac{1}{2} \leftarrow 1\frac{1}{2}$	$1 \leftarrow 0$	26.74	-1.4	1.278	-1.27
+ +	$1\frac{1}{2} \leftarrow 1\frac{1}{2}$	-1	31.87[d]	-1.1	2.557	-1.05
+ +	$1\frac{1}{2} \leftarrow 1\frac{1}{2}$	0	32.42[d]	-0.8	2.557	-1.05
+ +	$1\frac{1}{2} \leftarrow 1\frac{1}{2}$	1	32.92[d]	-0.7	2.557	-1.05
+ +	$\frac{1}{2} \leftarrow \frac{1}{2}$	-1	88.11[d]	0.4	2.557	-0.42
+ +	$\frac{1}{2} \leftarrow \frac{1}{2}$	0	88.62[d]	0.6	2.557	-0.42
. + +	$\frac{1}{2} \leftarrow \frac{1}{2}$	1	89.14[d]	0.9	2.557	-0.42
. + -	$1\frac{1}{2} \leftarrow 1\frac{1}{2}$	-1	252.40[d]	-0.6	2.557	-1.16
. + -	$1\frac{1}{2} \leftarrow 1\frac{1}{2}$	0	253.38[d]	-0.6	2.557	-1.16
. + -	$1\frac{1}{2} \leftarrow 1\frac{1}{2}$	1	254.34[d]	-0.8	2.557	-1.16
. + -	$\frac{1}{2} \leftarrow \frac{1}{2}$	e	501.3	-5.2	0.0	-0.74
+ +	$-\frac{1}{2} \leftarrow -\frac{1}{2}$	e	930.03	-0.9	2.557	-0.36
. + -	$-\frac{1}{2} \leftarrow -\frac{1}{2}$	e	1403.06	-0.7	2.557	-0.59
1 polarisation (σ)						
. + +	$\frac{1}{2} \leftarrow 1\frac{1}{2}$	e	26.74	0.1	2.557	-1.27
. + +	$-\frac{1}{2} \leftarrow \frac{1}{2}$	1	56.91[d]	0.5	2.557	-0.61
+ +	$-\frac{1}{2} \leftarrow \frac{1}{2}$	0	57.40[d]	0.6	2.557	-0.61
+ +	$-\frac{1}{2} \leftarrow \frac{1}{2}$	-1	57.85[d]	0.9	2.557	-0.61
+ +	$1\frac{1}{2} \leftarrow \frac{1}{2}$	-1	190.05[d]	-0.1	2.557	-0.22
+ +	$1\frac{1}{2} \leftarrow \frac{1}{2}$	0	192.98[d]	0.1	2.557	-0.22
+ +	$1\frac{1}{2} \leftarrow \frac{1}{2}$	1	195.84[d]	0.2	2.557	-0.22
. + -	$\frac{1}{2} \leftarrow 1\frac{1}{2}$	-1	207.82[d]	-0.4	2.557	-1.42
. + -	$\frac{1}{2} \leftarrow 1\frac{1}{2}$	0	208.25[d]	-0.5	2.557	-1.42
. + -	$\frac{1}{2} \leftarrow 1\frac{1}{2}$	1	208.65[d]	-0.9	2.557	-1.42
. + -	$-\frac{1}{2} \leftarrow \frac{1}{2}$	e	380.36	-4.3	2.557	-0.90
. + -	$1\frac{1}{2} \leftarrow \frac{1}{2}$	-1	845.53	-0.6	2.557	-0.48
. + -	$1\frac{1}{2} \leftarrow \frac{1}{2}$	0	847.46	-0.6	2.557	-0.48
. + -	$1\frac{1}{2} \leftarrow \frac{1}{2}$	1	849.43	-0.5	2.557	-0.48

$26.4~\mu m$ *spectrum* $N = 2$, $J = 2\frac{1}{2} \leftarrow N = 1$, $J = 1\frac{1}{2}$

1 polarisation (π)						
+ + -	$-1\frac{1}{2} \leftarrow -1\frac{1}{2}$	-1	274.38[d]	-0.3	1.647	0.62
+ + -	$-1\frac{1}{2} \leftarrow -1\frac{1}{2}$	0	274.49[d]	-0.1	1.647	0.62
+ + -	$-1\frac{1}{2} \leftarrow -1\frac{1}{2}$	1	274.61[d]	0.0	1.647	0.62
+ + -	$-\frac{1}{2} \leftarrow -\frac{1}{2}$	-1	433.92[d]	-0.8	1.647	0.52

<div align="center">TABLE IV—Continued</div>

parity	M_J	M_I^a	Flux Density (mT)	$\nu_{laser} - \nu_{calc}$ (MHz)	Wt^b (MHz^{-2})	$\partial\nu/\partial B$ (MHz/...
+ ← −	−½ ← −½	0	434.09^d	−0.7	1.647	0.52
+ ← −	−½ ← −½	1	434.30^d	−0.8	1.647	0.52
− ← +	−1½ ← −1½	e	439.02^d	−0.1	1.647	0.73
− ← +	−½ ← −½	−1	628.84^d	−0.2	1.647	0.65
− ← +	−½ ← −½	0	629.05^d	−0.3	1.647	0.65
− ← +	−½ ← −½	1	629.25^d	−0.3	1.647	0.65
+ ← −	½ ← ½	e	849.34	−0.1	1.647	0.43
− ← +	½ ← ½	−1	1104.26^d	−0.2	1.647	0.51
− ← +	½ ← ½	0	1104.71^d	−0.2	1.647	0.51
− ← +	½ ← ½	1	1105.13^d	0.0	1.647	0.51

⊥ polarisation (σ)

parity	M_J	M_I^a	Flux Density (mT)	$\nu_{laser} - \nu_{calc}$ (MHz)	Wt^b (MHz^{-2})	$\partial\nu/\partial B$ (MHz/...
+ ← −	−½ ← −1½	e	131.36^d	−0.3	1.647	1.17
+ ← −	½ ← −½	−1	175.50^d	−0.1	1.647	0.91
+ ← −	½ ← −½	0	175.77^d	−0.2	1.647	0.91
+ ← −	½ ← −½	1	176.00^d	0.1	1.647	0.91
− ← +	−½ ← −1½	e	222.10	0.0	1.647	1.25
+ ← −	1½ ← ½	−1	273.36^d	0.2	1.647	0.60
+ ← −	1½ ← ½	0	273.68^d	0.2	1.647	0.60
+ ← −	1½ ← ½	1	274.00^d	0.2	1.647	0.60
− ← +	½ ← −½	e	292.11	0.2	1.647	0.99
− ← 1	1½ ← ½	−1	447.02^d	−0.9	1.647	0.67
− ← +	1½ ← ½	0	447.22^d	−1.0	1.647	0.67
− ← +	1½ ← ½	1	447.43^d	−1.1	1.647	0.67
+ ← −	2½ ← 1½	−1	844.80^d	−0.6	1.647	0.18
+ ← −	2½ ← 1½	0	845.63^d	−0.7	1.647	0.18
+ ← −	2½ ● 1½	1	846.45^d	−0.8	1.647	0.18
− ← +	2½ ← 1½	−1	1422.46^d	−0.1	1.647	0.19
− ← +	2½ ← 1½	0	1423.37^d	−0.3	1.647	0.19
− ← +	2½ ● 1½	1	1424.23^d	−0.3	1.647	0.19
+ ← −	−1½ ← −½	−1	1812.49^d	−0.8	1.647	0.50
+ ← −	−1½ ← −½	0	1813.01^d	−0.8	1.647	0.50
+ ← −	−1½ ← −½	1	1813.54^d	−0.8	1.647	0.50

218.3 μm spectrum $N = 3$, $J = 3½$ and 2½ ← $N = 2$, $J = 2½$

‖ polarisation (π)

parity	M_J	M_I^a	Flux Density (mT)	$\nu_{laser} - \nu_{calc}$ (MHz)	Wt^b (MHz^{-2})	$\partial\nu/\partial B$ (MHz/...
− ← +	−2½ ← −2½	−1	945.29^d	1.6	1.060	0.51
− ← +	−2½ ← −2½	0	946.62^d	1.7	1.060	0.51
− ← +	−2½ ← −2½	1	947.93^d	1.9	1.060	0.51

⊥ polarization (σ)

parity	M_J	M_I^a	Flux Density (mT)	$\nu_{laser} - \nu_{calc}$ (MHz)	Wt^b (MHz^{-2})	$\partial\nu/\partial B$ (MHz/...
− ← +	1½ ← ½	e	1410.14	3.2	1.060	1.42
+ ← −	1½ ← ½	e	1460.35	2.0	1.060	1.44
− ← +	−1½ ← −2½	−1	1530.2	1.3	1.060	0.23
− ← +	−1½ ← −2½	0	1532.2	0.9	1.060	0.23
− ← +	−1½ ← −2½	1	1533.6	1.8	1.060	0.23

TABLE IV—*Continued*

parity	M_J	M_I[a]	Flux Density (mT)	$\nu_{laser}-\nu_{calc}$ (MHz)	Wt[b] (MHz^{-2})	$\partial\nu/\partial B_0$[c] (MHz/G)

$215.4\ \mu m$ *spectrum* $N = 3,\ J = 2\frac{1}{2} \leftarrow N = 2,\ J = 1\frac{1}{2}$

∥ polarisation (π)

- ← +	$-2\frac{1}{2} \leftarrow -1\frac{1}{2}$	$1 \leftarrow 0$	8.18[d]	−0.3	0.516	0.54
- ← +	$-1\frac{1}{2} \leftarrow -1\frac{1}{2}$	1	8.18[d]	−0.3	0.516	0.44
- ← +	$-2\frac{1}{2} \leftarrow -1\frac{1}{2}$	$0 \leftarrow 1$	8.85[d]	−0.5	1.032	0.61
- ← +	$-1\frac{1}{2} \leftarrow -1\frac{1}{2}$	0	9.89[d]	−0.4	1.032	0.52
- ← +	$-1\frac{1}{2} \leftarrow -1\frac{1}{2}$	−1	11.15[d]	−0.6	1.032	0.53
- ← +	$-\frac{1}{2} \leftarrow -1\frac{1}{2}$	$-1 \leftarrow 0$	13.40[d]	−0.4	1.032	0.38
- ← +	$-1\frac{1}{2} \leftarrow -\frac{1}{2}$	$1 \leftarrow 0$	18.11[d]	−0.1	1.032	0.27
- ← +	$-1\frac{1}{2} \leftarrow -\frac{1}{2}$	$0 \leftarrow -1$	18.60[d]	−0.2	1.032	0.30
- ← +	$-\frac{1}{2} \leftarrow -\frac{1}{2}$	1	30.11[d]	−0.1	1.032	0.14
- ← +	$-\frac{1}{2} \leftarrow -\frac{1}{2}$	0	32.16[d]	−0.2	1.032	0.14
- ← +	$-\frac{1}{2} \leftarrow -\frac{1}{2}$	−1	34.18[d]	−0.3	1.032	0.15
- ← +	$-\frac{1}{2} \leftarrow -\frac{1}{2}$	−1	398.62[d]	−1.1	1.032	−0.12
- ← +	$-\frac{1}{2} \leftarrow -\frac{1}{2}$	0	400.13[d]	−1.1	1.032	−0.12
- ← +	$-\frac{1}{2} \leftarrow -\frac{1}{2}$	1	401.80[d]	−0.8	1.032	−0.13
- ← +	$-2\frac{1}{2} \leftarrow -2\frac{1}{2}$	e	970.24	3.0	1.032	1.79
+ ← -	$-2\frac{1}{2} \leftarrow -2\frac{1}{2}$	−1	1104.21[d]	3.0	1.032	1.83
+ ← -	$-2\frac{1}{2} \leftarrow -2\frac{1}{2}$	0	1104.50[d]	2.9	1.032	1.83
+ ← -	$-2\frac{1}{2} \leftarrow -2\frac{1}{2}$	1	1104.76[d]	3.3	1.032	1.83
- ← +	$-1\frac{1}{2} \leftarrow -1\frac{1}{2}$	−1	1421.94[d]	−0.8	1.032	0.88
- ← +	$-1\frac{1}{2} \leftarrow -1\frac{1}{2}$	0	1422.11[d]	−0.3	1.032	0.88
- ← +	$-1\frac{1}{2} \leftarrow -1\frac{1}{2}$	1	1422.26[d]	0.4	1.032	0.88
- ← +	$-1\frac{1}{2} \leftarrow -1\frac{1}{2}$	−1	1500.89[d]	2.5	1.032	−0.13
- ← +	$-1\frac{1}{2} \leftarrow -1\frac{1}{2}$	0	1504.57[d]	2.6	1.032	−0.12
- ← +	$-1\frac{1}{2} \leftarrow -1\frac{1}{2}$	1	1508.33[d]	2.6	1.032	−0.12
+ ← -	$-1\frac{1}{2} \leftarrow -1\frac{1}{2}$	e	1682.62	0.4	1.032	0.84

$215.4\ \mu m$ *spectrum* $N = 3,\ J = 2\frac{1}{2} \bullet N = 2,\ J = 1\frac{1}{2}$

⊥ polarisation (σ)

- ← +	$-2\frac{1}{2} \leftarrow -1\frac{1}{2}$	1	6.64[d]	0.3	1.032	0.52
- ← +	$-2\frac{1}{2} \leftarrow -1\frac{1}{2}$	0	7.08[d]	0.2	1.032	0.58
- ← +	$-2\frac{1}{2} \leftarrow -1\frac{1}{2}$	−1	7.95[d]	−0.1	1.032	0.64
- ← +	$-1\frac{1}{2} \leftarrow -1\frac{1}{2}$	$0 \leftarrow 1$	8.35[d]	0.0	1.032	0.53
- ← +	$-1\frac{1}{2} \leftarrow -1\frac{1}{2}$	$-1 \leftarrow 0$	9.17[d]	0.3	1.032	0.52
- ← +	$-1\frac{1}{2} \leftarrow -1\frac{1}{2}$	$0 \leftarrow 1$	13.08[d]	−0.2	1.032	0.39
- ← +	$-\frac{1}{2} \leftarrow -1\frac{1}{2}$	−1	15.57[d]	0.5	1.032	0.38
- ← +	$-1\frac{1}{2} \leftarrow -\frac{1}{2}$	1	16.95[d]	−0.4	1.032	0.27
- ← +	$-1\frac{1}{2} \leftarrow -\frac{1}{2}$	−1	17.50[d]	−0.5	1.032	0.30
+ ← -	$-2\frac{1}{2} \leftarrow -1\frac{1}{2}$	e	435.66	−0.1	1.032	0.40
- ← +	$-1\frac{1}{2} \leftarrow -2\frac{1}{2}$	−1	731.78[d]	4.0	1.032	1.96
- ← +	$-1\frac{1}{2} \leftarrow -2\frac{1}{2}$	0	732.08[d]	3.8	1.032	1.96
- ← +	$-1\frac{1}{2} \leftarrow -2\frac{1}{2}$	1	732.38[d]	3.5	1.032	1.96
- ← +	$-1\frac{1}{2} \leftarrow -\frac{1}{2}$	e	826.32[d]	−1.2	1.032	−0.23
+ ← -	$-1\frac{1}{2} \leftarrow -2\frac{1}{2}$	e	838.58[d]	3.5	1.032	2.00
- ← +	$-\frac{1}{2} \leftarrow -1\frac{1}{2}$	e	989.89	1.5	1.032	1.19
- ← +	$-1\frac{1}{2} \leftarrow -\frac{1}{2}$	e	1161.14	0.9	1.032	1.15
- ← +	$\frac{1}{2} \leftarrow -\frac{1}{2}$	e	1555.73	0.1	1.032	0.60

TABLE IV—*Continued*

parity	M_J	M_I[a]	Flux Density (mT)	$\nu_{laser} - \nu_{calc}$ (MHz)	Wt[b] (MHz^{-2})	$\partial\nu/\partial B_o$[c] (MHz/G)

163.0 μm spectrum $N = 4 \leftarrow 3$, *both spin components*

‖ polarisation (π)

parity	M_J	M_I	Flux Density	$\nu_{laser}-\nu_{calc}$	Wt	$\partial\nu/\partial B_o$
+ ← −	−3½ ← −3½	−1	635.37[d]	0.3	0.5915	0.58
+ ← −	−3½ ← −3½	0	636.45[d]	0.5	0.5915	0.58
+ ← −	−3½ ← −3½	1	637.27[d]	2.2	0.5915	0.58
− ← +	3½ ← 3½	1	1484.20[d]	−1.1	0.5915	−0.04
− ← +	3½ ← 3½	0	1486.8[d]	−1.1	0.5915	−0.04
− ← +	3½ ← 3½	−1	1489.5[d]	−0.9	0.5915	−0.04

⊥ polarisation (σ)

parity	M_J	M_I	Flux Density	$\nu_{laser}-\nu_{calc}$	Wt	$\partial\nu/\partial B_o$
− ← +	2½ ← 3½	e	346.86	−2.7	0.5915	−0.34
− ← +	1½ ← 2½	e	439.84[d]	−2.2	0.5915	−0.24
− ← +	½ ← 1½	1	659.54[d]	−2.2	0.5915	−0.12
− ← +	½ ← 1½	0	660.21[d]	−2.3	0.5915	−0.12
− ← +	½ ← 1½	−1	660.98[d]	−2.3	0.5915	−0.12
+ ← −	−2½ ← −3½	e	1114.6	−2.1	0.5915	0.21

129.5 μm spectrum　$N = 5 \leftarrow 4$, *both spin components*

‖ polarisation (π)

parity	M_J	M_I	Flux Density	$\nu_{laser}-\nu_{calc}$	Wt	$\partial\nu/\partial B_o$
+ ← −	−2½ ← −2½	e	310.0	−6.3	0.3735	0.43
− ← +	−3½ ← −3½	e	413.8	−2.6	0.3735	0.91
+ ← −	−3½ ← −3½	e	613.3	−3.9	0.3735	1.36
− ← +	−4½ ← −4½	−1	743.55	6.5	0.3735	2.47
− ← +	−4½ ← −4½	0	744.03	6.2	0.3735	2.47
− ← +	−4½ ← −4½	1	744.53	5.6	0.3735	2.46
+ ← −	−4½ ← −4½	−1	956.29	4.4	0.3735	2.46
+ ← −	−4½ ← −4½	0	956.66	3.0	0.3735	2.46
+ ← −	−4½ ← −4½	1	956.96	3.2	0.3735	2.46

⊥ polarisation (σ)

parity	M_J	M_I	Flux Density	$\nu_{laser}-\nu_{calc}$	Wt	$\partial\nu/\partial B_o$
− ← +	−4½ ← −3½	−1	107.9	−6.6	0.3735	−1.53
− ← +	−4½ ← −3½	0	108.7	−6.4	0.3735	−1.53
− ← +	−4½ ← −3½	1	109.6	−4.7	0.3735	−1.53
+ ← −	−3½ ← −2½	e	484.1	−2.8	0.3735	1.04
− ← +	−4½ ← −3½	−1	546.69[d]	1.0	0.3735	1.49
− ← +	−4½ ← −3½	0	546.83[d]	1.0	0.3735	1.49
− ← +	−4½ ← −3½	1	546.99[d]	0.6	0.3735	1.49
− ← +	−3½ ← −4½	e	672.40	2.0	0.3735	2.48
+ ← −	−4½ ← −3½	−1	753.41[d]	0.2	0.3735	1.74
+ ← −	−4½ ← −3½	0	753.71[d]	0.3	0.3735	1.74
+ ← −	−4½ ← −3½	1	754.00[d]	0.5	0.3735	1.74
+ ← −	−3½ ← −4½	e	860.9	3.6	0.3735	2.47

TABLE IV—*Continued*

parity	M_J	M_I[a]	Flux Density (mT)	$\nu_{laser} - \nu_{calc}$ (MHz)	Wt[b] (MHz^{-2})	$\partial\nu/\partial B_0$[c] (MHz/G)

108.8 µm spectrum, $N = 6 \leftarrow 5$, both spin components

∥ polarisation (π)

parity	M_J	M_I	Flux Density (mT)	$\nu_{laser}-\nu_{calc}$	Wt	$\partial\nu/\partial B_0$
+ ← −	−5½ ← −5½	−1	46.28	−1.7	0.2635	2.34
+ ← −	−5½ ← −5½	0	46.86	−1.6	0.2635	2.34
+ ← −	−5½ ← −5½	1	47.42	−0.8	0.2635	2.34
+ ← −	−4½ ← −4½	−1	60.19[d]	−0.7	0.2635	1.67
+ ← −	−4½ ← −4½	0	60.83[d]	−0.9	0.2635	1.66
+ ← −	−4½ ← −4½	1	61.42[d]	−0.1	0.2635	1.66
+ ← −	−3½ ← −3½	e	93.90	−2.5	0.0	0.78
+ ← −	−3½ ← −3½	1	246.54[d]	−1.1	0.2635	−0.75
+ ← −	−3½ ← −3½	0	246.79[d]	−1.0	0.2635	−0.75
+ ← −	−3½ ← −3½	−1	247.02[d]	−1.1	0.2635	−0.76
+ ← −	−4½ ← −4½	−1	401.86[d]	−2.6	0.2635	−1.56
+ ← −	−4½ ← −4½	0	402.07[d]	−2.6	0.2635	−1.55
+ ← −	−4½ ← −4½	1	402.30[d]	−2.2	0.2635	−1.55
− ← +	−5½ ← −5½	e	587.00[d]	−4.7	0.2635	0.31

108.8 µm spectrum $N = 6 \leftarrow 5$, both spin components

⊥ polarisation (σ)

parity	M_J	M_I	Flux Density (mT)	$\nu_{laser}-\nu_{calc}$	Wt	$\partial\nu/\partial B_0$
+ ← −	−4½ ← −5½	−1	50.40	4.3	0.2635	2.09
+ ← −	−4½ ← −5½	0	51.10	1.6	0.2635	2.09
+ ← −	−4½ ← −5½	1	51.60	3.2	0.2635	2.09
+ ← −	−3½ ← −4½	e	69.3	−1.9	0.2635	1.37
+ ← −	−4½ ← −3½	e	300.58	−2.2	0.2635	−1.14
+ ← −	−3½ ← −4½	e	365.20	−2.5	0.2635	−1.31
+ ← −	−5½ ← −4½	e	442.1	−4.5	0.2635	−1.82

4.3. Determination of Molecular Parameters

The data in Table IV were used to determine an optimal set of molecular parameters for CD in the $v = 0$ level of the $X\,^2\Pi$ state. The Hamiltonian used was the N^2 version described by Brown *et al.* (25). Since CD in its ground state conforms almost exactly to Hund's case (b), we have determined combinations of parameters appropriate to this limit. For example, the lambda-doubling parameters p and q are better determined than the case (a) combinations $(p + 2q)$ and q. Since it is not possible to determine both the parameters A_D and γ in a fit of a single species in a $^2\Pi$ state, we have performed the fit with the former constrained to zero. Consequently the parameters determined as A and γ take effective values, denoted by a tilde (e.g., $\tilde{A}$) in our results. The combination of these values with those for CH allow the parameters A_D and γ to be separated, as we discuss in the next section.

The basis set was truncated without loss in accuracy at $\Delta N = \pm 1$, consistent with the Hund's case (b) behavior. Each datum was weighted in the fit inversely as the

BROWN AND EVENSON

square of the estimated experimental error; the weights are given in Table IV. The error comes partly from the uncertainty in the knowledge of the far-infrared laser frequencies ($\sim 5 \times 10^{-7}$) and partly from the uncertainty in the magnetic flux measurements.

The results of the fit are given in Table IV and the parameter values determined in the process are given in Table V. Some of the smaller parameters had to be constrained to values estimated from other sources. These are indicated in the table. The electron spin g-factor is estimated to have a value of 2.0020, corresponding to a relativistic correction of 1.5×10^{-4}. All the other constrained parameters were obtained by scaling from the corresponding value of CH. It was assumed that the electric quadrupole interaction at the D nucleus would be too small to be determinable. The standard

TABLE V

Parameters for CD in the $v = 0$ Level of the $X\,^2\Pi$ State[a]

$\tilde{A}$	$842308.65(34)$[b]	B	$230896.199(46)$
$\tilde{\gamma}$	$-423.802(86)$	D	$12.8218(14)$
$10\gamma_D$	0.732[c]	$10^3 H$	0.4751[c]
p	$544.44(22)$	q	$339.418(68)$
$10p_D$	$-0.58(15)$	$10q_D$	$0.765(27)$
$10^5 p_H$	0.52[c]	$10^5 q_H$	0.835[c]
a	$8.05(36)$	c	$8.85(67)$
b_F	$-8.92(37)$	d	$7.11(31)$
$g_L{}'$	$1.000661(76)$	$10^2 g_r$	$-0.1560(16)$
g_S	2.0020[c]	$10^2 g_e$	0.1178
$10^2 g_\ell$	0.1010[c]	$10^2 g_r{}^{e\,'}$	-0.147

[a] Value in MHz, where appropriate.

[b] The numbers in parenthesis represent 1 standard deviation of the least-squares fit, in units of the last quoted digit.

[c] Parameter constrained to this value in the least-squares fit.

deviation of the fit relative to the experimental uncertainty is 1.526, a figure which can be regarded as reasonably satisfactory (a value of 1.0 is expected if the model is adequate and the weighting factors have been chosen correctly).

4. DISCUSSION

This paper describes the measurement and analysis of the far-infrared LMR spectrum of the CD free radical in the lowest vibrational level of the $X^2\Pi$ state. All the data have been fitted satisfactorily to within experimental error. As a result, the spin-rotational energy levels of CD are now very much better defined.

The parameter values determined in the fit are given in Table V. The value for the rotational constant B_0 can be related to that for CH (12, 7) assuming that the vibrational dependence is given simply by

$$B_v = B_e - \alpha_e(v + \tfrac{1}{2}) + \gamma_e(v + \tfrac{1}{2})^2. \tag{6}$$

Bernath (10), using the same N^2 Hamiltonian, has determined the values for α_e and γ_e of ^{12}CH to be 16 014 (17) and 59.4 (45) MHz, respectively. Assuming simple isotopic scaling factors for B_e, α_e, and γ_e, we obtain a value of 230 527 MHz for B_0 of CD, in reasonably good agreement with the experimental value of 230 896 MHz. The discrepancy between these values has two causes. First, the vibrational dependence assumed in Eq. (6) may be inadequate for such a light molecule. Second, the isotopic dependence of B_e is more complicated than a simple proportionality to μ^{-1} (26) where μ is the reduced mass. The additional correction terms can be determined once the vibrational dependence of B_v is better defined for CD by the study of the molecule in vibrationally excited levels.

It is also possible to compare the spin–orbit coupling constants A_0 for CH and CD. First, however, it is necessary to remove the effects of the constraint $A_D = 0$ on these parameters. The parameter determined in the fit, $\hat{A}$, is related to A by (27)

$$\hat{A} = A\{1 + A_D/2B\}. \tag{7}$$

The spin–rotation constant $\hat{\gamma}$ is also an effective parameter, having absorbed the effects of A_D on the energy levels.

$$\hat{\gamma} = \gamma - A_D(A - 2B)/2B. \tag{8}$$

Brown and Watson (17) have shown that it is possible to separate the parameters γ and A_D on the right-hand side of Eq. (8) by exploiting their isotopic dependencies. Using this procedure with the parameters for CH and CD in their ground vibrational levels, we obtain

$$A_D = 17.67 \text{ MHz}, \qquad \gamma = -771.3 \text{ MHz} \qquad \text{for CH}$$

and

$$A_D = 9.53 \text{ MHz}, \qquad \gamma = -415.8 \text{ MHz} \qquad \text{for CD}.$$

It is of interest to note that γ has a much larger effect on the energy levels than A_D. This is the normal behavior. Also the value of $\hat{\gamma}$ for CH is almost exactly equal to the true value γ. This follows from Eq. (8) when it is realized that $A \simeq 2B$ for CH.

Once the value for A_D has been determined, it becomes possible to determine the

"true" values of the spin–orbit coupling constants from Eq. (7). The values obtained are 843 800.0 MHz for CH and 842 291.3 MHz for CD, both in the $v = 0$ level. If we accept a simple vibrational dependence for A_v, namely

$$A_0 = A_e - \tfrac{1}{2}\alpha_A, \tag{9}$$

we can use the difference of the A_0 values to determine α_A for CH. Assuming A_e and $\alpha_A \mu^{-1/2}$ to be isotopically independent, we obtain a value for α_A for CH of -11.3 GHz. This is in very poor agreement with the value determined by Bernath (10) of -5.783 GHz. A similarly poor estimate of α_A was obtained from a combination of A_0 values for OH and OD (27). It is probable that the assumed isotopic dependencies of A_e and α_A are oversimplistic and that other nonadiabatic corrections similar to those described by Watson for the mechanical parameters (26) are required when dealing with data of the present precision.

It can be seen from Table V that we have determined the four principal magnetic hyperfine parameters for the deuteron in CD (the electric quadrupole parameters are almost certainly too small to be determined). These should scale accurately from those of CH in the ratio of the nuclear g-factors, that is, dividing by a factor of 6.5144. Scaling the best available values for CH (7), we obtain for CD

$$a = 8.40 \text{ MHz}, \qquad c = 8.93 \text{ MHz}$$
$$b_F = -8.83 \text{ MHz}, \qquad d = 6.674 \text{ MHz}.$$

These values are in good agreement with those obtained independently for CD, shown in Table V.

The other parameter for CD which can be usefully compared with that for CH is the rotational g-factor, g_r. There are nuclear and electronic contributions to this g-factor but both should scale as μ^{-1}. The ratio of g_r for CH to that for CD is 1.803(33), in good agreement with the expected value of 1.8550.

The results of the present work should aid the detection of CD in interstellar space.

TABLE VI

The Calculated Lambda-Doubling Spectrum of the CD Radical in Its Ground State

J	F$_1$			F$_2$	
1/2				$-$ ← $+$	1222.9 MHz
3/2	$+$ ← $-$	685.7 MHz		$+$ ← $-$	1757.8
5/2	$+$ ← $-$	416.3		$-$ ← $+$	4076.1
7/2	$-$ ← $+$	2179.2		$+$ ← $-$	7048.8
9/2	$+$ ← $-$	4607.0		$-$ ← $+$	10677.7
11/2	$-$ ← $+$	7694.3		$+$ ← $-$	14955.4

Estimated 1σ uncertainty = 1.5 MHz.

TABLE VII

Calculated Spin–Rotation Transition Frequencies for the CD Radical in Its Ground State[a]

N' – N''	Transition J' – J''	parity	Frequency (GHz)	Vacuum Wavelength (μm)	Line Strength[b]
		ΔN = 1, ΔJ = 1 transitions			
2 – 1	2½ – 1½	– ← +	915.854	327.3365	2.1108
		+ ← –	916.956	326.9431	2.1122
3 – 2	3½ – 2½	+ ← –	1379.674	217.2923	3.2017
		– ← +	1381.437	217.0150	3.2028
4 – 3	4½ – 3½	– ← +	1840.529	162.8838	4.2587
		+ ← –	1842.957	162.6693	4.2596
5 – 4	5½ – 4½	+ ← –	2299.507	130.3725	5.2976
		– ← +	2302.594	130.1977	5.2983
6 – 5	6½ – 5½	– ← +	2756.682	108.7512	6.3257
		+ ← –	2760.421	108.6039	6.3263
2 – 1	1½ – ½	– ← +	1325.261	226.2140	0.3794
		+ ← –	1325.796	226.1223	0.3816
3 – 2	2½ – 1½	+ ← –	1389.603	215.7397	1.8272
		– ← +	1391.921	215.3803	1.8285
4 – 3	3½ – 2½	– ← +	1845.841	162.4151	3.0622
		+ ← –	1848.813	162.1540	3.0633
5 – 4	4½ – 3½	+ ← –	2302.892	130.1809	4.1754
		– ← +	2306.521	129.9761	4.1762
6 – 5	5½ – 4½	– ← +	2759.068	108.6571	5.2421
		+ ← –	2763.346	108.4889	5.2427
		ΔN = 1, ΔJ = 0 transitions			
2 – 1	1½ – 1½	– ← +	884.775	338.8346	0.2193
		+ ← –	887.219	337.9014	0.2158
3 – 2	2½ – 2½	+ ← –	1358.524	220.6751	0.1593
		– ← +	1362.184	220.0822	0.1568
4 – 3	3½ – 3½	– ← +	1824.691	164.2977	0.1224
		+ ← –	1829.561	163.8604	0.1205
		ΔN = 0, ΔJ = 1 transitions			
1 – 1	1½ – ½	+ ← –	439.262	682.4905	0.9517
		– ← +	439.800	681.6570	0.9539

[a] Calculated with parameters from Table V. Hyperfine splittings have been suppressed. Estimated 1σ uncertainty = 3 MHz.
[b] The line strength is defined in Eq. (10).

For the convenience of radio astronomers, we list the calculated values of the lambda-doubling intervals in the first few rotational levels of CD in Table VI. We estimate these values to have an uncertainty (1σ) of 1.5 MHz. For further reference, we give the far-infrared rotational spectrum of CD in Table VII, computed from the parameter values in Table V. In this case, the frequencies are reliable to about 3 MHz. The line strengths of the transitions are also given in Table VII. The line strength $S_{J'J''}$ can be used to assess the relative intensity of an individual zero-field transition. It is defined by

$$S_{J'J''} = |\langle \gamma'J'||D_q^{(1)}(\omega)^*||\gamma''J''\rangle|^2, \tag{10}$$

where the quantity on the right-hand side is the reduced matrix element of the rotation matrix (29) and γ stands for subsidiary quantum numbers. The intensity of a line in absorption can be obtained by multiplying the line strength by the square of the dipole moment, by the transition frequency, and by the population difference factor between the two levels.

The present work is confined to a study of CD in its ground vibrational level. Much further work remains in exploring the molecule in excited vibrational levels. Many far-infrared LMR spectra of vibrationally excited CD have been recorded and the analysis is in an advanced state. We have also detected lines in the fundamental band of the vibration–rotation spectrum of CD by CO laser magnetic resonance. The result of this work will be reported in due course.

REFERENCES

1. G. HERZBERG, "Spectra of Diatomic Molecules," Van Nostrand, Princeton, NJ, 1950.
2. J. E. BUTLER, J. W. FLEMING, L. P. GOSS, AND M. C. LIN, *Chem. Phys.* **56**, 355–365 (1981).
3. W. J. MILLER, "Fourteenth Symposium (International) on Combustion," p. 307, The Combustion Institute, Pittsburgh, 1973.
4. W. W. DULEY AND D. A. WILLIAMS, "Interstellar Chemistry," Academic Press, London, 1984.
5. L. GERÖ, *Z. Phys.* **118**, 27–36 (1941).
6. G. HERZBERG AND J. W. C. JOHNS, *Astrophys. J.* **158**, 399–418 (1969).
7. C. R. BRAZIER AND J. M. BROWN, *Canad. J. Phys.* **62**, 1563–1578 (1984).
8. W. UBACHS, G. MEYER, J. J. TER MEULEN, AND A. DYMANUS, *J. Chem. Phys.* **84**, 3032–3041 (1986).
9. K. G. LUBIC AND T. AMANO, *J. Chem. Phys.* **81**, 1655–1660 (1984).
10. P. F. BERNATH, *J. Chem. Phys.* **86**, 4838–4842 (1987).
11. J. T. HOUGEN, J. A. MUCHA, D. A. JENNINGS, AND K. M. EVENSON, *J. Mol. Spectrosc.* **72**, 463–478 (1978).
12. J. M. BROWN AND K. M. EVENSON, *J. Mol. Spectrosc.* **98**, 392–403 (1983).
13. M. BOGEY, C. DEMUYNCK, AND J. L. DESTOMBES, *Chem. Phys. Lett.* **100**, 105–109 (1983).
14. T. C. STEIMLE, D. R. WOODWARD, AND J. M. BROWN, *J. Chem. Phys.* **85**, 1276–1282 (1986).
15. S. A. DAVIDSON, K. M. EVENSON, AND J. M. BROWN, in preparation.
16. L. GERÖ, *Z. Phys.* **117**, 709–721 (1941).
17. J. M. BROWN AND J. K. G. WATSON, *J. Mol. Spectrosc.* **65**, 65–74 (1977).
18. T. J. SEARS, P. R. BUNKER, A. R. W. MCKELLAR, K. M. EVENSON, D. A. JENNINGS, AND J. M. BROWN, *J. Chem. Phys.* **77**, 5348–5362 (1982).

P. R. BUNKER, T. J. SEARS, A. R. W. McKELLAR, K. M. EVENSON, AND F. J. LOVAS, *J. Chem. Phys.* **79**, 1211–1219 (1983).

K. M. EVENSON, T. J. SEARS, AND A. R. W. McKELLAR, *J. Opt. Soc. Amer. B.* **1**, 15–21 (1984).

E. HILL AND J. H. VAN VLECK, *Phys. Rev.* **32**, 250–272 (1928).

C. H. TOWNES AND A. L. SCHAWLOW, "Microwave Spectroscopy." McGraw-Hill, New York, 1955.

J. T. HOUGEN, "The Calculation of Rotational Energy Levels and Rotational Line Intensities in Diatomic Molecules," p. 49, Monograph 15, National Bureau of Standards, Washington DC, 1970.

R. N. ZARE, A. L. SCHMELTEKOPF, W. J. HARROP, AND D. L. ALBRITTON, *J. Mol. Spectrosc.* **46**, 37–66 (1973).

J. M. BROWN, E. A. COLBOURN, J. K. G. WATSON, AND F. D. WAYNE, *J. Mol. Spectrosc.* **74**, 294–318 (1979).

J. K. G. WATSON, *J. Mol. Spectrosc.* **80**, 411–421 (1980).

J. M. BROWN AND J. E. SCHUBERT, *J. Mol. Spectrosc.* **95**, 194–212 (1982).

M. INGUSCIO, G. MORUZZI, K. M. EVENSON, AND D. A. JENNINGS, *J. Appl. Phys.* **60**, R161–R192 (1986).

D. M. BRINK AND G. R. SATCHLER, "Angular Momentum," Oxford Univ. Press, Oxford, 1968.